

5-2009

Characterization of amino acid adlayers on InAs surfaces using X-ray photoelectron spectroscopy

John W. Slavin

Purdue University - Main Campus, jslavin@purdue.edu

Upasana Jarori

Purdue University - Main Campus, ujarori@purdue.edu

Dmitry Zemlyanov

Purdue University - Main Campus, dimazemlyanov@purdue.edu

Albena Ivanisevic

Birck Nanotechnology Center, Purdue University, albena@purdue.edu

Follow this and additional works at: <http://docs.lib.purdue.edu/nanopub>



Part of the [Nanoscience and Nanotechnology Commons](#)

Slavin, John W.; Jarori, Upasana; Zemlyanov, Dmitry; and Ivanisevic, Albena, "Characterization of amino acid adlayers on InAs surfaces using X-ray photoelectron spectroscopy" (2009). *Birck and NCN Publications*. Paper 565.

<http://docs.lib.purdue.edu/nanopub/565>

This document has been made available through Purdue e-Pubs, a service of the Purdue University Libraries. Please contact epubs@purdue.edu for additional information.



Characterization of amino acid adlayers on InAs surfaces using X-ray photoelectron spectroscopy

John W.J. Slavin^a, Upasana Jarori^b, Dmitry Zemlyanov^c, Albena Ivanisevic^{a,b,*}

^a Department of Chemistry, Purdue University, West Lafayette, IN 47907, USA

^b Weldon School of Biomedical Engineering, Purdue University, West Lafayette, IN 47907, USA

^c Birck Nanotechnology Center, Purdue University, West Lafayette, IN 47907, USA

ARTICLE INFO

Article history:

Available online 24 March 2009

Keywords:

SAM
InAs
XPS
Amino acid

ABSTRACT

Removal of surface oxide layers and the prevention of their reformation is an essential step in the use of III-V semiconductor technologies. Highlighted here are data exploring the use of amino acid (AA) self-assembled monolayers (SAMs) to block the pre-growth of oxides on indium arsenide surfaces. Three different AAs were used: lysine, aspartic acid, and cysteine. The adlayers were characterized by atomic force microscopy (AFM), Raman, and angle resolved X-ray photoelectron spectroscopy (ARXPS). AFM data suggest that the AA functional groups affect the packing and orientation of the molecules on the surfaces, reinforced by contact angle data. Raman data provide proof that the type of functional group alters the intensity of the unscreened LO phonon, resulting in an electrostatic stabilization, in the case of lysine, which lends to the case of electrostatic interactions blocking oxide formation. ARXPS demonstrated that the degree of oxide blocking is dependent upon the type of functional group and further verifies inferences made from the Raman spectra. The degree of monolayer formation is also determined from this data. It is concluded that AA's can be useful means for blocking oxide growth on InAs (1 0 0) surfaces, which also provides insights into how protein and peptide side chains might interact with such surfaces.

© 2009 Elsevier B.V. All rights reserved.

1. Introduction

Understanding of semiconductor surface chemistry is essential for the creation of functional devices for electronic applications. In many cases, the flow of electrons from the bulk semiconductor materials can be controlled by altering the surface properties [1–3]. In order for specific properties of these materials to be exploited, the electronic transfer must be protected from undesired chemical alterations such as atmospheric oxidation [4,5]. Much work has been accomplished using IV-IV, III-V, and II-VI semiconductors to ensure that particular properties are protected. In some cases this has been accomplished by the formation of self-assembled monolayers (SAMs) on these surfaces [5–9]. An added benefit of this approach is that the application of the SAMs also allows for co-interactions to be achieved between the bulk semiconductor material and the end-groups on the monolayers (MLs). This phenomenon lends the potential for new device development based upon chosen interactions [10,11].

Indium arsenide (InAs), a III-V semiconducting material, has found utility in infrared detection and high-speed transistors, and

its further use has been extended to the fabrication of quantum dots with specific photoluminescence properties [12]. InAs is known to be passivated by thioacetamide (TAM), inorganic sulfide of the form $(\text{NH}_4)_2\text{S}_x$ and the formation of self-assembled monolayers bonded through thiol end-groups [12–14]. In addition, InAs stands out among semiconducting materials in that the conduction band is below the Fermi level in the (1 0 0) and (1 1 1) oriented crystals, a property which makes it to nearly acts as a conductor rather than semiconductor [15,16]. This property results in there being a surface charge accumulation region filled with a two-dimensional electron gas; however, there has yet to be an observed occupied surface state above the valence-band maximum (VBM), resulting in the material being classified as semiconducting and non-metallic in nature [12,17,18]. In order to fully understand the means by which these surface properties affect surface bound groups and the latter, it is of interest to further probe the passivation of InAs by thiols, as in the previously described methods, and to examine the co-interactions seen with the incorporation of other chemical functionalities.

In this paper we investigate the chemical bonding properties of three amino acids (AAs) on InAs surfaces. Cysteine (Cys), lysine (Lys), and aspartic acid (Asp) were applied to the surface, either from neat methanol solutions or from solutions containing butylamine as an additive. In order to examine the effects of solvent conditions, additional samples, made under the same experimental method, were analyzed, including: MeOH only, MeOH/butylamine,

* Corresponding author at: Weldon School of Biomedical Engineering, Purdue University, 206 S. Martin Jischke Drive, West Lafayette, IN 47907, USA.

E-mail address: albena@purdue.edu (A. Ivanisevic).

butylamine (BuAm), Lys only, and Asp only. Surface properties were examined by taking contact angle measurements, Raman spectra, atomic force microscopy (AFM), and X-ray photoelectron spectroscopy (XPS) data. The ability of these amino acids to bond or absorb to the surface is discussed, including information on the degree of monolayer formation. Importantly, the results are analyzed to determine which functionalities allow to passivate the surface, thereby preventing atmosphere oxidation. Functional group interactions are further verified primarily by XPS analysis. We present evidence that Cys is able to form covalent bonds to indium with a significant decrease in oxide thickness. We also show that the nitrogen content, in the form of amines and imines, positively affects passivation of InAs (1 0 0) surface.

2. Experimental

2.1. Substrates and chemicals

Un-doped single-polished (1 0 0) oriented indium arsenide, InAs (1 0 0), substrates were purchased from University Wafer (South Boston, MA). Crystalline amino acids and 99% bromine were acquired from Sigma–Aldrich. 1 cm × 1 cm sections of the wafers were sonicated in water, methanol, and ethanol for 15 min. Sonicated samples were etched in a 0.1% bromine solution in methanol for approximately 3 min. Subsequently all pieces were sonicated in each solvent for an additional 5 min after etching, and finally dried under N₂.

2.2. Sample preparation

Samples were prepared by boiling the etched pieces of InAs (1 0 0) in methanol solutions of each amino acid type. Cys solutions were prepared by grinding the crystals with a mortar and pestle and then boiling 60.0 mg of the powder in 100 mL of methanol. Lys and Asp solutions were prepared similarly, with the exception that stoichiometric quantities of butylamine (C₄H₉NH₂) were added to aid in the dissolution of the amino acids. In each system, InAs chips were boiled for 15 min while keeping the solution at 100 mL by the addition of methanol. After boiling, the samples were sonicated for an additional 5 min in each solvent, then dried with N₂.

2.3. Contact angle measurements

As received, etched, and functionalized surfaces were examined to determine hydrophobicities using a Tanteq, Inc. CAM-PLUS contact angle meter. Measurements were performed on each type of surface a minimum of five times, and angles were determined using the half-angle method.

2.4. Atomic force microscopy

Etched and modified samples were imaged by a Digital Instruments Multi-Mode Nanoscope IIIa Atomic Force Microscope (AFM) using single beam cantilevers from Veeco Instruments, CA (model code: OTESPA7). Scan sizes ranged from 2 to 4 μm with roughness values being calculated from 2 μm × 2 μm sized images. A scan rate of 2 Hz was used for all samples. Surface roughness values from a given surface were determined using the Nanoscope III 5.12r3 software package, from a minimum of five images.

2.5. Raman spectroscopy

Samples were examined on a Horiba Jobin Yvon HR800 Spectrometer using a 100×/0.90 Olympus MPlan objective. During experiments the grating was set at 600. Peaks were normalized

based upon the signal intensity, which was a function of the focusing of the beam, and was performed prior to averaging the data sets for each type of sample. An average of 5 data sets per type of sample was used for determining peak intensities. Data acquisition and raw analysis was performed using Labspec 5.25.15 software package.

2.6. X-ray photoelectron spectroscopy

X-ray photoelectron spectroscopy data was collected by a Kratos Ultra DLD spectrometer using an Al Kα monochromic X-ray radiation. The high resolution spectra of the In 3d and 4d, As 2p_{3/2} and 3d, C 1s, N 1s, and S 2s and 2p core levels were collected at photoemission angles between 0 and 60°, with respect to the surface normal, at fixed analyzer pass energy of 20 eV. Survey scans were performed at 0° with pass energy of 160 eV. The charge shift was calibrated to the C 1s peak at 284.8 eV, resulting in standard deviation of ±0.05 eV as related to the calibration method. Data analysis was performed using the CasaXPS software package, version 2.3.12. Curve-fitting was done after subtraction of the Linear, Shirley, or Tougaard type background assuming Gaussian/Lorentzian line shape.

Angle resolved XPS (ARXPS) were performed at photoemission angles of 0, 30, 45, and 60° on each sample surface. In order to calculate the thickness values, quantitative electron attenuation lengths (Q_{EAL}) and average electron attenuation lengths (L_{ave}) were calculated using the National Institution of Standards and Technology (NIST) Standard Reference Database 82: Electron Effective Attenuation Length Database (Ver. 1.1). These values were calculated for As 2p_{3/2}, As 3d, In 3d, and In 4d photoemission peaks assuming that photoelectrons travel through ideal InAs. Additionally, to understand carbon contamination on the surfaces, Q_{EAL} s were calculated for hexane as an estimation of the average type of carbon contaminant expected. The band gap used in the NIST software to calculate Q_{EAL} was chosen to be 6.0 eV. In order to determine the values for an oxide film an estimation method was used based upon empirical data from these experiments. It was found that a fraction of arsenic atoms had been removed from the near-surface region. The XPS obtained ratio of In:As was used to estimate oxide band gap and density for oxide film.

3. Results and discussion

III-V semiconducting surfaces have recently been investigated as possible components for biologically inspired devices, yet at the current time little is known as to the response that these materials may have when interacting with certain biologically relevant compounds. Upon SAM formation, side chains of proteins and peptides may lend to symbiotic effects between the surface and the protein/peptide's structure. Side chains could enable passivation of semiconducting surfaces, while controlled orientation of the molecules could enable proper access of substrates to active sites. Examining the interactions between the simplest components of proteins and peptides, or the individual AA's, and semiconducting surfaces could provide useful information with regard to how larger systems would interact with the same surfaces. This study specifically examines the removal of oxide layers from InAs (1 0 0) surfaces, and the ability of AA's to passivate the crystal surface.

Most semiconductor passivation experiments begin with the etching of a surface oxide layer to reveal the underlying crystal surface. Examining the physical effects of wet etching is necessary to determine the degree to which this process affects the surfaces. InP and InAs (1 0 0) are known to have pit formation upon etching of their native oxides [19–21]. These pits are reported to be between the submicron and micron size ranges, and in some instances are observable even by the naked eye. This effect leads to an increase in surface roughness upon etching with Br₂. Applying AA's to these

Table 1

Roughness and contact angle values after the surfaces were treated with different adsorbates. Averages were determined based upon at least 5 data sets.

Surface	Surface roughness, R_a (nm)	Contact angle ($^\circ$)
Unetched	0.22 ± 0.0	47.6 ± 2.0
Etched	0.54 ± 0.1	25.7 ± 0.8
Cysteine	0.94 ± 0.2	33.1 ± 0.5
Aspartic acid	0.58 ± 0.1	22.1 ± 0.7
Lysine	0.75 ± 0.1	51.4 ± 3.0

surfaces lead to an increase in the surface roughness, with the degree of change depending upon the compound used. Table 1 reports the observed changes in roughness as a result of etching and functionalization, as well as the contact angle changes.

Roughness data suggests that AA functional groups vary the orientations and packing of the molecules on the semiconductor surfaces. In the case of this study, the differences in roughness observed are related to both the quantity of AA's attached to the surfaces as well as to the depletion of arsenic from the surface (as discussed below), a result of the etching and functionalization procedure. From the contact angle data it is apparent that AA functional groups cause a specific change in hydrophobicity on the surfaces. The aspartic acid samples' low contact angle suggests that at least one carboxyl group is away from the surface. The increase in angle for the lysine layers is an indication of amine interactions with the water droplets. Amine terminated surfaces generally have contact angles of $\sim 67^\circ$ so there is evidence for a carboxyl interaction as well [22,23]. The hydrophilic nature of the cysteine modified surface suggests an even more pronounced interaction with the carboxylic acid group on the SAM surface pointing towards possible binding between the surface and the amine group, as well as the expected chemisorbed sulfur bond to the substrate.

Fig. 1 presents Raman results providing an initial qualitative assessment of the degree of oxide removal. As mentioned above, peaks were normalized due to changes in beam focusing. This normalization was achieved by fitting the peak at 225 cm^{-1} to a standard maximum y-axis value. Previous reports have suggested that the 249 cm^{-1} peak in the material's Raman spectrum originate from the charge accumulation regions unscreened LO phonon [24]. The greater the intensity of the 249 cm^{-1} peak, the more the surface is oxidized. Examining the ratio of the oxide peak to the reference InAs (1 0 0) signal at 225 cm^{-1} provides information about whether oxide has been removed during the treatment process, and may lend to time dependent information on the reformation of the oxide layers [12]. The currently described Raman method does not provide accurate quantitative data due to the lack of resolution seen between the oxide and InAs (1 0 0) reference peaks.

It may be surmised in this experiment that the ledge at $\sim 250 \text{ cm}^{-1}$ correlates to the 239 cm^{-1} LO phonon, with the peak at $\sim 220 \text{ cm}^{-1}$ corresponding to the 225 cm^{-1} phonon–plasmon mode. This estimate is made since Tanzer et al. used a wavelength of 457.9 nm to probe the surface characteristics of the InAs (1 0 0) surfaces [12], while the instrument used in the described research was set at 600 nm . This difference is the source for the broadening of the peaks as well as the decrease in intensity for the LO phonon as opposed to the previously described research. The change is insignificant for current purposes since, as can be noted from Fig. 1, there is still a net decrease in the 249 cm^{-1} ledge of the spectrum upon etching. Though this difference is observed, only semi-quantitative descriptions of the change in oxide thicknesses are described. Fully resolved peaks, obtained by altering the grating, would provide a more reliable description than the current one. Regardless, the decrease in intensity of the 249 cm^{-1} protuberance corresponds to the change in LO phonon, and thus the pinning of the Fermi level, quantified by calculating the ratio between it and the 220 cm^{-1} peak [25]. The ratio of the peaks can roughly be

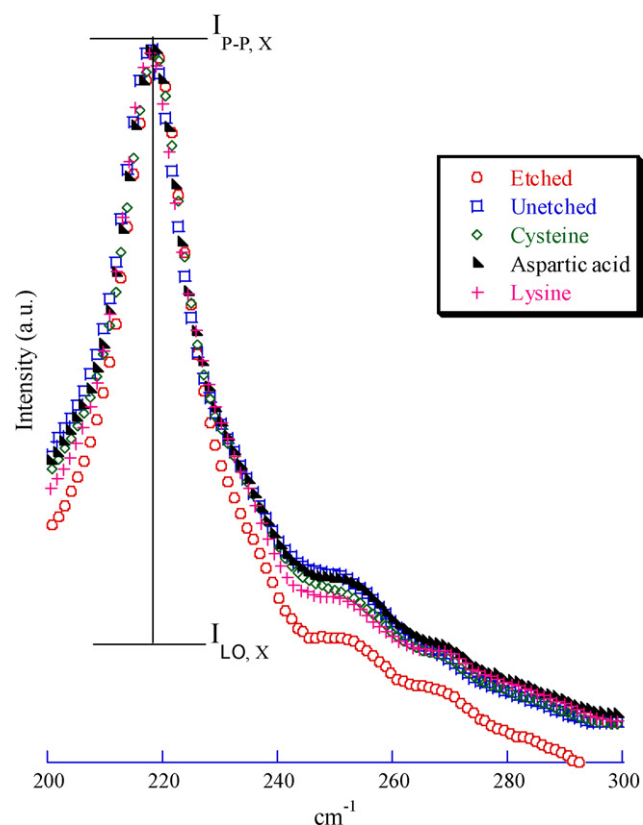


Fig. 1. Raman spectrum of phonon–plasmon mode at 220 cm^{-1} and LO phonon of 250 cm^{-1} . The change in the LO phonon corresponds to the degree of surface oxidation. Red circles are for etched surfaces, blue boxes for unetched, green diamonds for cysteine, black triangles for aspartic acid, and pink plus signs for lysine. (For interpretation of the references to color in this figure legend, the reader is referred to the web version of the article.)

related to the efficiency of oxide removal and passivation through the following relationship:

$$\text{Eff} (\%) = \frac{R_{\text{Unetched}} - R_{\text{Sample}}}{R_{\text{Unetched}} - R_{\text{Etched}}} \times 100 \quad (1)$$

which describes the quantity of oxide removed as related to the etched and unetched samples. R refers to the ratio of the intensities between the LO phonon and the phonon–plasmon mode (P–P) peaks [12]. The top half of the equation describes the difference in oxidation between the sample and the unetched reference, while the bottom half describes the total observed change in intensity upon etching. The values from this equation are reported in Table 2 as percentage of oxide removed in relation to the unetched sample. It is clear from the ratios that the difference between the unetched and functionalized samples is negligible, thus statistically insignificant; however with further qualification this could provide another means of verifying the removal of oxide species from semiconductor surfaces. It would also be of interest to expand upon the Raman based methods to further describe the possible functional

Table 2

Change in intensity of the LO phonon peak relative to the height of the phonon–plasmon peak. Ratios are calculated in respect to oxide thicknesses on an etched and unetched standard using Eq. (1).

Sample	Ratio (ILO/IP-P)	Oxide thickness (%)
Unetched	0.465	100
Etched	0.401	0
Cysteine	0.451	22.2
Lysine	0.433	34.7
Aspartic acid	0.46	7.8

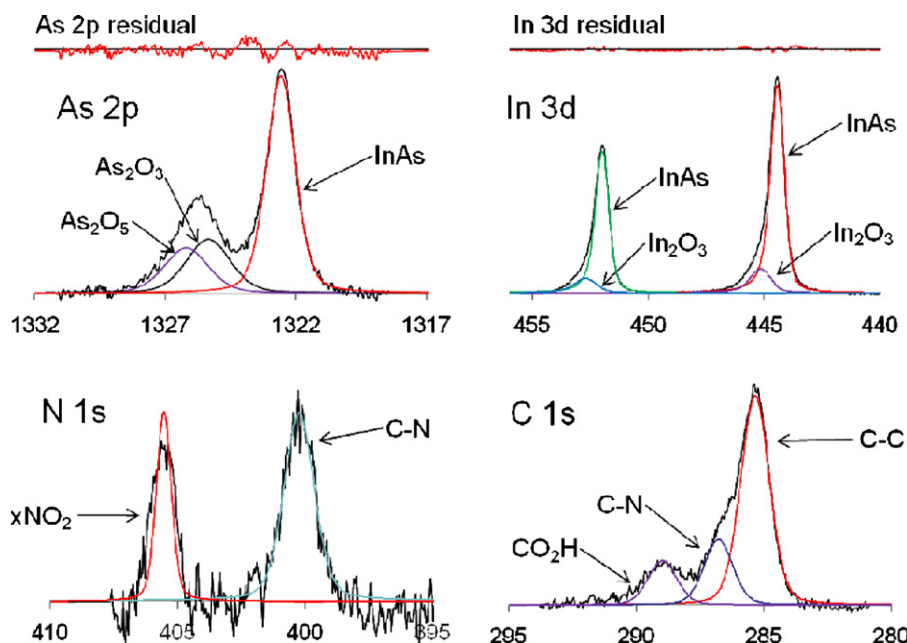


Fig. 2. High resolution XPS spectra of the As 2p, In 3d, N 1s and C 1s region of the InAs (1 0 0) after it was functionalized with Cys.

group interactions to support XPS oxide thickness calculations as are described below.

The capability of AAs to passivate surface oxidation was explored using ARXPS. This technique is based on varying the photoemission angle and by doing this the surface sensitivity can be tuned. Thus, at steep photoemission angles, the spectra are more surface sensitive, whereas at normal photoemission (0°) the sensitivity towards bulk composition is maximized and surface contribution is minimized. ARXPS allowed us to calculate thicknesses of both oxide layers and adsorbed layers. XPS data can also be used to calculate a fractional coverage, which is measured in monolayers, ML, and represents the ratio between the number of adsorbed species and the number of surface atoms of substrate. As an example, the core-level XPS spectra obtained from cysteine adlayer are shown in Fig. 2.

As it was reported in the literature, semiconductors containing As were observed to have a depletion of arsenic upon etching or subsequent exposure to passivating solutions [5,25]. The same occurred in our experiments. It was determined that $41.0 \pm 1.0\%$ of arsenic atoms had been removed from the near-surface region. From this depletion, the density of the oxide was calculated by taking the sum of the densities of In_2O_3 and As_2O_3 multiplied by 0.625 and 0.375, respectively. The band gap for the oxide was calculated in the same manner. Coverages of AA adsorbed layers on the InAs (1 0 0) surface are shown in Table 3. These values were calculated as the number of carbon or nitrogen per indium atom normalized for the number of carbon (nitrogen) atoms in AA molecule. 1 monolayer (ML) corresponds to a 1:1 ratio between the number of surface species and crystal atoms. There have been similar discussions of surface layer depletions where X-ray induced damage occurs, yet this was not readily observed in our experiments [26].

The method for calculating the coverage, thickness, and oxide thickness has been described before [6,27]. Briefly, coverage was determined by the non-attenuating adlayer approximation [6,27] using the equation:

$$\theta = \frac{I_{C/N}}{I_{\text{In/As}}} \frac{Q_{\text{EAL}}(E_{\text{In/As}}) \cos \alpha}{dN} \quad (2)$$

where $Q_{\text{EAL}}(E_{\text{In/As}})$ is the attenuation length for photoelectrons emitted from a certain electron level for the substrate, α is the photoemission angle, d is distance between closest plane of In/As, which

is half the lattice constant for InAs (1 0 0), N is the number of C or N atoms per AA molecule, $I_{x,y}$ refers to the peak areas corrected to the relative sensitivity factor (RSF), which accounts for the Reilman asymmetric parameter, β , and Scofield differential cross-sections. It is important to note that the depletion of arsenic introduces an error in the value of d since the lattice changes when these atoms are removed. A correction could be applied in this case, yet there is no way of finding an accurate means of estimating the change in the lattice constant without examining the crystal structure of the altered surfaces. Examples of the C 1s and N 1s spectra used to determine the coverage are presented in Fig. 3.

The thickness of adsorbed AA layer can be estimated from the attenuation of the substrate's photoelectron flux, due to an electron travel through adlayers as:

$$I = I_0 \exp\left(-\frac{t}{L_{\text{ave}} \cos \alpha}\right) \quad (3)$$

Here I_0 and I are intensities of photoelectron peaks from clean and adsorbate coated substrate, respectively. Eq. (3) can be reformulated as:

$$\ln\left(\frac{I}{I_0}\right) = -\frac{t}{L_{\text{ave}} \cos \alpha} \quad (4)$$

and t/L_{ave} can be obtained by plotting $\ln(I/I_0)$ versus $1/\cos \alpha$.

Table 3

Coverage of AA layers on InAs (1 0 0) surfaces. Coverage values were calculated based upon the quantity of carbon or nitrogen per indium atom.

Experiment	Sample	Coverage C	Coverage N
1	Etched	1.8	1.1
1	MeOH	3.0	1.1
1	BuAm	1.8	0.4
1	BuAm MeOH	2.1	0.8
1	Lysine MeOH	1.1	0.4
1	Lysine BuAm MeOH	1.1	0.4
1	Aspartic acid MeOH	1.3	2.0
1	Aspartic acid BuAm MeOH	0.6	0.6
1	Cysteine MeOH	2.1	1.6
2	Etched	2.2	0.8
2	Cysteine MeOH	3.1	3.2
2	Arginine MeOH	0.9	0.7
2	Glutamic acid BuAm MeOH	0.7	1.2

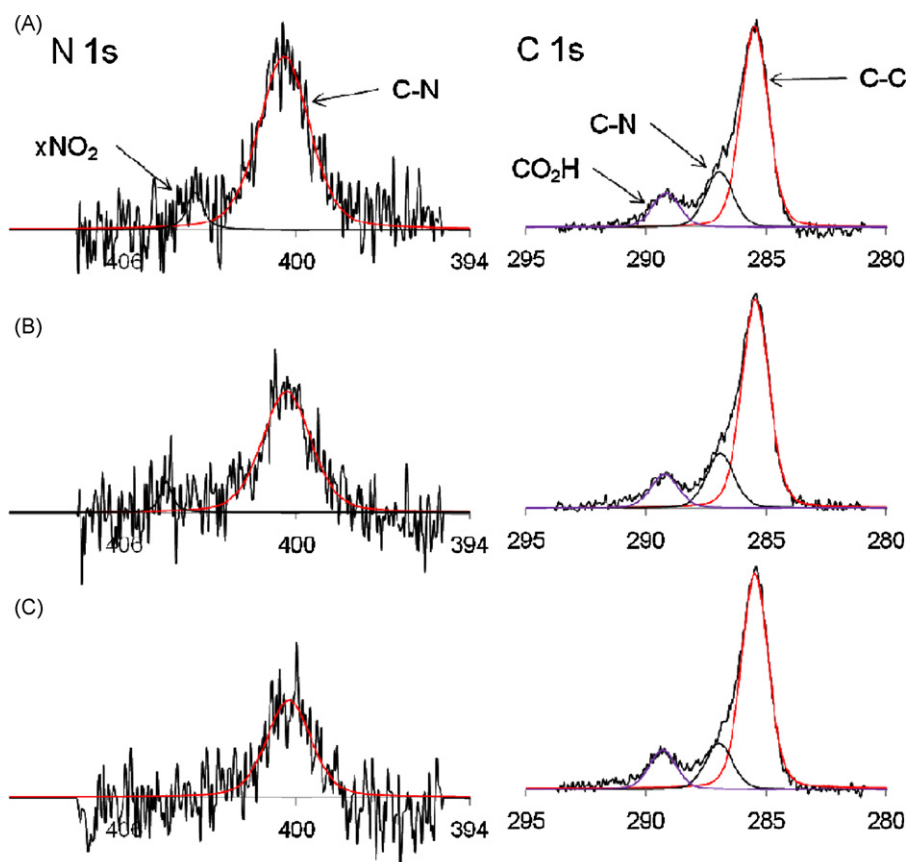


Fig. 3. The C 1s and N 1s spectra used to calculate surface coverage. The spectra were obtained from (A) lysine-butyl amine functionalized, (B) aspartic acid-butyl amine functionalized, and (C) butyl amine treated surfaces. C 1s spectra adjacent to N 1s spectra are for the same AA.

A comparison between the oxide thicknesses calculated based on Raman and XPS data can be made. From the Raman, the maximum decrease in LO phonon intensity, and thus oxide, is around 34% from the Lys samples; while the minimum was 8.8% for Asp. The XPS suggests a 32–50% decrease in oxide layer thickness upon treatment with Cys or Arg, while the remaining amino acids only resulted in a 29% oxide removal or smaller (Table 4).

Comparing the Lys samples with and without BuAm addition, a marked decrease in oxide thickness is observed upon introducing BuAm. There is evidence that the inability of the neat Lys solution to cause the same degree of passivation has less to do its potential to passivate than it does with dissolution of the AA during the process. Lys is observed to dissolve in the solution containing BuAm whereas in pure methanol solutions it remains largely crystalline. To be sure that the solvating agent is not causing this

increase in passivation one may look to the MeOH treated surface and the MeOH/BuAm surface where there is only a slight change in oxide thickness between the two. Treating the surfaces with BuAm does result in a decrease in oxide thickness, yet when examined in other systems, for instance when added to the Asp treatment, no appreciable change occurs. This does not suggest that BuAm only functions as a dissolution agent when involved in the AA systems, as apparent from its bulk effects on the surfaces, but it does show that it possibly has less effect when used as an additive.

Functional groups possessed by each AA are the dominant factor governing their interactions with the substrates. In the case of Asp there is evidence for an interaction between the molecule's carboxyl groups and the surface. Taking into consideration the small decrease in LO phonon intensity affected by the AA, there seems to be an electrostatic binding of Asp to the positively charged indium

Table 4

Oxide thickness calculated for different AA adlayer based on In 3d, As 2p_{3/2} and As 3d. Oxide thickness was calculated for 0° photoemission.

Experiment	Sample	Thickness (Å) based on In 3d	Oxide thickness (Å) based on As 2p _{3/2}	Oxide thickness (Å) based on As 3d
1	Etched	10.0	4.0	4.2
1	MeOH	9.9	2.8	2.9
1	BuAm	6.9	2.6	2.4
1	BuAm MeOH	10.0	3.1	3.3
1	Lysine MeOH	6.9	4.0	4.2
1	Lysine BuAm MeOH	7.2	3.1	3.2
1	Aspartic acid MeOH	10.3	2.9	3.0
1	Aspartic acid BuAm MeOH	6.9	2.9	3.0
1	Cysteine MeOH	8.8	2.3	2.4
2	Etched	14.8	3.6	3.8
2	Cysteine MeOH	13.7	1.7	1.7
2	Arginine MeOH	10.0	2.1	2.2
2	Glutamic acid BuAm MeOH	8.7	2.5	2.6

atoms. Since this binding would further promote charge accumulation at the interface one would expect to see an increase in the phonon, relative to the actual amount of oxide removed. The XPS suggests ~29% oxide removal with Asp, this destabilizing effect significantly shifts the LO phonon towards the unetched surfaces' LO position, as would be expected. There is some suggestion of this type of behavior seen with GaAs (100) substrate and molecules containing carboxyl groups, where the groups form coordination complexes with the gallium, a result of a strong acid interaction [25]. In order to explore further the possibility of the similar physisorption, glutamic acid (Glu) was examined, in the presence of BuAm (since no significant difference was seen between the Asp and Asp/BuAm samples), as another possible passivation agent. XPS results suggest that Glu passivation functions similarly to Asp, forming comparably packed layers and blocking similar quantities of sites on the surface.

There is a correlation observed between nitrogen content in the AA's used and the degree of passivation achieved. The ability of N–H groups to bond to In containing semiconductor surfaces has been previously reported [28–30]. Since BuAm did affect the degree of passivation with the Lys monolayers, there seems to be a relationship between amine groups and passivation ability. It is important to explore this in order to ensure that passivation is not solely the result of the boiling process in MeOH, where coordination of methoxide ions with indium could be leading to the prevention of atmospheric oxidation [31–33]. In order to further characterize the possible amine interactions, Arg layered samples were prepared by boiling in a 1 mM methanoic Arg solution. Increasing the nitrogen content per molecule did result in increased passivation of the InAs (100) surface. The question remains why the amine groups in BuAm and Lys, when added in equal quantities, do not lead to such a degree in passivation as well. Unfortunately it is not clear from the data taken whether the species are chemisorbed or physisorbed in the Lys and Arg samples, which would give a clear indication of surface interactions. An electrostatic interaction with lysine in this case is expected to be able to occur between amine groups and either surface In or As. There are reports in similar systems that nitrogen groups electrostatically bind to the V element of the III–V dichotomy [34]. We expect in the case of InAs (100) surfaces, this interaction is weaker than in the case of InP, but still possible. There are other suggestions, which in the absence of electrochemical potentials seem most likely, that amine groups attack the III element as a Lewis base [35,36]. There have been studies to determine the role of competing groups in the past from which similar studies might be drawn [37]. It may be presumed though, that electrostatic interactions play the largest role in the observed systems. Under regular conditions Arg and BuAm both have pK_a values of ~12.5, while Lys's pK_a is slightly lower at 10.5. The difference in pK_a between the guanidinium group in the Arg and amine in Lys could increase the interaction with the substrate enough to provide a meaningful change in passivation potential. This difference in pK_a may provide this aid, but it must be considered that at neutral pH all molecules will have a net charge of –1. If the interaction is electrostatic, this charge similarity leads to the main difference being the number of amine/imine groups each molecule possesses. For instance, the BuAm group may have a similar pK_a to Arg, but the fact that a quarter of the nitrogen content per molecule is available for surface interaction greatly decreases its ability to effectively block the oxidation.

The imine of Arg could also play a significant part in the surface passivation. Taken that the molecules are charged, the delocalization of charge in the imine, due to resonance, adds a degree of stability lacking in the amine containing molecules. This fact is reflected in the pK_a of the group. Since the additional nitrogen group of the imine is also able to interact with the surface, a more stable electrostatic binding is achieved. There could be, in all amine/imine

scenarios, the possibility of covalent bonding between As and N, or evidence in the As 2p or As 3d regions to suggest an As–N bond [38,39]. However now we do not have enough XPS data completely to rule out this scenario. This, in conjunction with the evidence from the Raman data, lends to the suggestion that the interaction is more than likely electrostatic and non-covalent in nature.

Another interesting trend is observed when comparing oxide thicknesses based upon the In 3d and 4d spectra, with those from the As 2p or 3d. The correlation between amino acid functional groups and oxide blocking seems to be related to the type of surface element that a moiety would interact with, in this case either a III or V semiconductor. Examining the data, AAs containing additional carboxyl groups tend to block oxidation of In better than they do oxidation of As. The opposite is true for molecules containing additional amines. This seems to further suggest a charge based interaction with the elements, as Asp and Glu would tend to be more negatively charged, thus interacting with the more positive In, while Lys and Arg would be more positive and prone to bind to As. Additional examination of these systems show Lys, BuAm, and Arg all decreasing the effectiveness of attempts to block In oxidation, while the Asp and Glu layers tend to have no negative effect on As. The reason for these observations has to do with In being able to serve only as a Lewis acid, while As may act as either Lewis base or acid. This explains the ability of the carboxyl containing AAs to still prevent oxidation of As on par with the amine containing AAs, since As is able to interact with either cationic or anionic species [40–42].

The ability to use AAs as passivation agents also depends upon their ability to form stable monolayers on surfaces. The values reported for coverages correspond to the number of monolayers formed on the respective surfaces, based upon the ratio between the surface substrate atoms to adsorbed molecules. As can be seen, most AAs used are able to form coverages close to a monolayer, with the exception of Cys, which tends to form multilayers. Correlated to this, Cys was shown to covalently bond to the surface. The quantity of bonding S in these experiments was significantly lower than that of the free thiol, which further supports the formation of multilayers. In all cases there was a large amount of carbon contamination seen on the surfaces, since 40–60% of the carbon signal for an individual AA was not from the deposited molecules. The thickness calculations correspond well with the predicted lengths of the AAs, with the exception of the Asp and Glu treated surfaces, which tended to be higher than expected. Though the values normally correlated well, the fact that a large part of the signal was from contamination prevents accurate prediction of tilt angles of the AAs, as normally calculated from the thickness values. Experiments would also be improved when performed in UHV environments, forming more stable and ordered layers while also preventing atmospheric oxidation on freshly etched samples between the etch and deposition steps [43].

4. Summary

In conclusion, the ability for individual AAs to passivate InAs (100) has been examined. Treatment of the substrates with the AA's results in an insignificant change in surface roughness and contact angles correspond well to that expect from the molecules deposited. Raman spectroscopy was used to determine the degree of passivation by examining the decrease in the LO phonon from the InAs (100) surface. Possible charge based interactions from Lys amine groups led to a decrease in the LO phonon signal while Cys chemisorption also proved a good means of affecting the signal. XPS analysis showed that Cys and Glu provided the largest prevention in oxide reformation on the substrates, while evidence for nitrogen containing groups benefiting passivation was also displayed. AAs were able to form monolayers on the substrates that com-

pared reasonably to thicknesses expected for each molecule's size. It is suggested that these individual subunits of proteins and peptides can interact with surfaces in beneficial ways. This lends to the possibility of increasing the scope with which passivation may be included in other steps of biosensor device fabrication.

Acknowledgements

This work was supported by NSF under CHE-0614132. We thank Prof. Ozan Akkus for access to a Raman spectrometer.

References

- [1] N. Wu, Q. Zhang, C. Zhu, D.S.H. Chan, M.F. Li, N. Balasubramanian, A. Chin, D.L. Kwong, *Applied Physics Letters* 85 (2004) 4127.
- [2] Y. Dong, X.M. Ding, X.Y. Hou, Y. Li, X.B. Li, *Applied Physics Letters* 77 (2000) 3839–3841.
- [3] J.W. Osenbach, *Journal of the Electrochemical Society* 140 (1993) 3667–3675.
- [4] M.J. Lowe, T.D. Veal, C.F. McConville, G.R. Bell, S. Tsukamoto, N. Koguchi, *Surface Science* 523 (2003) 179–188.
- [5] V. Bessolov, M. Lebedev, *Semiconductors* 32 (1998) 1141–1156.
- [6] R. Flores-Perez, D.Y. Zemlyanov, A. Ivanisevic, *Journal of Physical Chemistry C* 112 (2008) 2147–2155.
- [7] M. Schwartzman, V. Sidorov, D. Ritter, Y. Paz, *Semiconductor Science and Technology* 16 (2001) L68–L71.
- [8] L. Xu, L. Wang, X. Huang, J. Zhu, H. Chen, K. Chen, *Low-Dimensional Systems and Nanostructures* 8 (2000) 129–133.
- [9] J. Roy, V.Y. Aristov, C. Radtke, P. Jaffrennou, H. Enriquez, P. Soukiassian, P. Moras, C. Spezzani, C. Crotti, P. Perfetti, *Applied Physics Letters* 89 (2006) 042114.
- [10] Y. Cho, A. Ivanisevic, *Langmuir* 22 (2006) 1768–1774.
- [11] P.G. Ganesan, A. Kumar, G. Ramanath, *Applied Physics Letters* 87 (2005) 011905.
- [12] T.A. Tanzer, P. Roshchin, L.H. Greene, J.F. Klem, *Applied Physics Letters* 75 (1999) 2794–2796.
- [13] D.Y. Petrovykh, J.P. Long, L.J. Whitman, *Applied Physics Letters* 86 (2005) 242105.
- [14] D.Y. Petrovykh, M.J. Yang, L.J. Whitman, *Surface Science* 523 (2003) 231–240.
- [15] D.C. Tsui, *Physical Review Letters* 24 (1970) 303–306.
- [16] S. Bhargava, H.R. Blank, V. Narayanamurti, H. Kroemer, *Applied Physics Letters* 70 (1997) 759–761.
- [17] L.Ö. Olsson, C.B.M. Andersson, M.C. Håkansson, J. Kanski, L. Ilver, U.O. Karlsson, *Physical Review Letters* 76 (1996) 3626–3629.
- [18] C.A. Mead, W.G. Spitzer, *Physical Review* 134 (1964) 713–716.
- [19] Z.F. Tomashik, S.G. Danylenko, V.N. Tomashik, M.Y. Kravetski, *Semiconductor Physics, Quantum Electronics & Optoelectronics* 2 (1999) 73–75.
- [20] M.F. Millea, M. McColl, A.H. Silver, *Journal of Electronic Materials* 5 (1976) 321–340.
- [21] G. Wagner, A. Dreilich, E. Butter, *Journal of Materials Science* 23 (1988) 2761–2767.
- [22] Y.P. Wang, K. Yuan, Q.L. Li, L.P. Wang, S.J. Gu, X.W. Pei, *Materials Letters* 59 (2005) 1736–1740.
- [23] S.J. Oh, S.J. Cho, C.O. Kim, J.W. Park, *Langmuir* 18 (2002) 1764–1769.
- [24] S. Buchner, E. Burstein, *Physical Review Letters* 33 (1974) 908–911.
- [25] S. Bastide, R. Butruille, D. Cahen, A. Dutta, J. Libman, A. Shanzer, L. Sun, A. Vilan, *Journal of Physical Chemistry B* 101 (1997) 2678–2684.
- [26] D. Zerulla, T. Chasse, *Langmuir* 15 (1999) 5285–5294.
- [27] C.S. Fadley, in: C.R. Brundle, A.D. Baker (Eds.), *Electron Spectroscopy: Theory, Techniques and Applications*, 1978, pp. 1–156.
- [28] L. Mohaddes-Ardabili, L.J. Martínez-Miranda, L.G. Salamanca-Riba, A. Christou, J. Silverman, W.E. Bentley, M. Al-Sheikhly, *Journal of Applied Physics* 95 (2004) 6021–6024.
- [29] L. Mohaddes-Ardabili, L.J. Martínez-Miranda, J. Silverman, A. Christou, L.G. Salamanca-Riba, M. Al-Sheikhly, W.E. Bentley, F. Ohuchi, *Applied Physics Letters* 83 (2003) 192–194.
- [30] R. Artzi, S.S. Daube, H. Cohen, R. Naaman, *Langmuir* 19 (2003) 7392–7398.
- [31] S.R. Lunt, G.N. Ryba, P.G. Santangelo, N.S. Lewis, *Journal of Applied Physics* 70 (1991) 7449–7467.
- [32] F. Ouyang, S. Yao, K. Tabata, E. Suzuki, *Applied Surface Science* 158 (2000) 28–31.
- [33] C.J. Carmalt, S.J. King, *Coordination Chemistry Reviews* 250 (2006) 682–709.
- [34] A.M. Gonçalves, O. Seitz, C. Mathieu, M. Herlem, A. Etcheberry, *Electrochemistry Communications* 10 (2007) 225–228.
- [35] L. Wang, L.P.F. Chibante, F.K. Tittel, R.F. Curl, R.E. Smalley, *Chemical Physics Letters* 172 (1990) 335–340.
- [36] C.R.C. Wang, A.M. DeSantolo, M.L. Mandich, J.W.D. Reents, *International Journal of Mass Spectrometry and Ion Processes* 130 (1994) 133–142.
- [37] D. Zerulla, I. Uhlig, R. Szargan, T. Chassé, *Surface Science* 402–404 (1998) 604–608.
- [38] R.L. Rowlands, S.J.C. Irvine, V. Barrioz, E.W. Jones, D.A. Lamb, *Semiconductor Science and Technology* 23 (2008) 15017.
- [39] J. Cui, M. Ozeki, M. Ohashi, *Applied Physics Letters* 71 (1997) 2659–2661.
- [40] K.J. Range, R. Ehrl, P. Hafner, *Journal of Alloys and Compounds* 240 (1996) 19–24.
- [41] H.G. Liu, J.Q. Wu, N. Tao, A.V. Firth, E.M. Griswold, T.W. MacElwee, C.R. Bolognesi, *Journal of Crystal Growth* 267 (2004) 592–597.
- [42] E.A. Piosos, B.S. Ault, *Journal of Physical Chemistry* 97 (1993) 3492–3496.
- [43] D. Zerulla, T. Chasse, *Langmuir* 18 (2002) 5392–5399.